

## Electronic Supplementary Information

for

### Relationship between crystal packing and high electron mobility in single crystal of thienyl-substituted methanofullerene

Jung Hei Choi,<sup>†</sup> Tatsuhiko Honda,<sup>†</sup> Shu Seki<sup>\*,‡</sup> and Shunichi Fukuzumi<sup>\*,†,§</sup>

<sup>†</sup>*Department of Material and Life Science, Graduate School of Engineering, Osaka University, ALCA, Japan Science and Technology Agency (JST), Suita, Osaka 565-0871, Japan*

<sup>‡</sup>*Department of Applied Chemistry, Graduate School of Engineering, Osaka University, Yamada-oka, Suita, Osaka 565-0871, Japan,* <sup>§</sup>*Department of Bioinspired Science, Ewha Womans University, Seoul 120-750, Korea*

\* To whom correspondence should be addressed.

E-mail: fukuzumi@chem.eng.osaka-u.ac.jp, seki@chem.eng.osaka-u.ac.jp

**X-ray Crystallographic Measurements.** Single crystals of ThCBM and PCBM were obtained by two-layered recrystallization with addition of ethanol on the top of the CS<sub>2</sub> solution of ThCBM, and addition of methanol on the top of the CS<sub>2</sub> solution of PCBM, respectively. The single crystals were mounted on glass capillaries with silicon grease. All measurements were performed on a Rigaku Mercury CCD area detector at -150 °C with graphite-monochromated MoK $\alpha$  radiation ( $\lambda = 0.71070 \text{ \AA}$ ) up to  $2\theta_{\text{max}} = 54.7^\circ$ . All calculations were performed using the Crystal Structure crystallographic software package,<sup>1</sup> and structure refinements were made by a direct method using SIR2004<sup>2</sup> for ThCBM and SIR97<sup>3</sup> for PCBM, respectively. Crystallographic data are summarized in Table 1. As for PCBM, methyl butanoate group is positionally disordered with 50% occupancy on each site. The two disordered -CH<sub>3</sub>C(O)OCH<sub>3</sub> groups were depicted in Fig. S1. (Group 1: C67, C83, O1, O2 and C79 and Group 2: C81, C80, O3, O4 and C82). The oxygen atom of O4 in the Group 2 and the carbon atom of C83 in the Group 1 occupied crystallographically the same position. For structural analysis, the electron density peak derived from these atoms was solely assigned to the carbon atom.

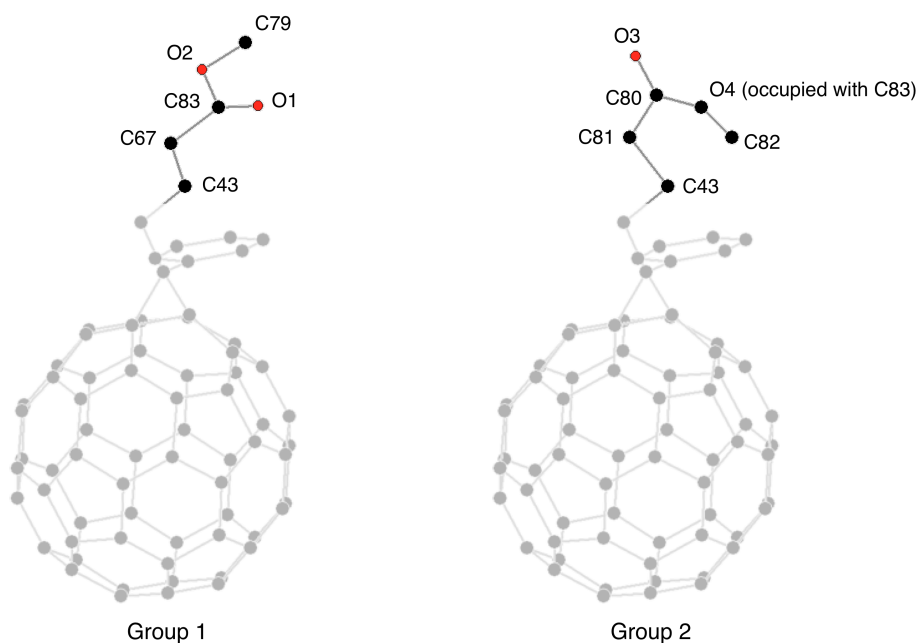


**Fig. S1** Disorder model of PCBM.

### Flash-Photolysis Time-Resolved Microwave Conductivity (FP-TRMC)

**Measurements.** The nanosecond laser pulses from a Nd: YAG laser (third harmonic generation, THG (355 nm) from Spectra Physics, INDY-HG (FWHM  $\sim 5$  ns) have been used as excitation sources with the power density of  $0.76 - 25 \text{ mJ/cm}^2$  ( $0.14 - 4.4 \times 10^{16}$  photons/ $\text{cm}^2$ ). Probing microwave frequency and power were set at  $\sim 9.1$  GHz and 3 mW, respectively. Absorbed power of the microwave in the cavity by local motion of photo-generated charge carriers was detected as the changes in electrical output of a sensing diode with the raise time of 1.5 ns, and monitored by a digital oscilloscope of Tektronix TDS3032B. All the above experiments were carried out at room temperature. Overall time constant of the present microwave circuit was  $10^{-7}$  s derived from the Q-value of the microwave cavity. The relative transient absorption of the microwave power reflected from the cavity ( $\Delta P_r/P_r$ ) was converted into the product of the sum of the mobilities of charge carriers ( $\Sigma\mu = \mu_+ + \mu_-$ : values of hole and electron mobilities) and the yield of photo-generated carriers ( $\phi$ ) as follows,

$$\Delta\sigma = \frac{1}{A} \frac{\Delta P_r}{P_r} = eN\phi \Sigma\mu \quad (1)$$

where  $A$ ,  $e$ ,  $\phi$ ,  $N$ , and  $\Sigma\mu$  are a sensitivity factor, elementary charge of electron, photo carrier generation yield (quantum efficiency), the number of absorbed photons per unit volume, and sum of mobilities for negative and positive carriers, respectively.<sup>4</sup> Polarization of the laser pulses is isotropic. ThCBM and PCBM crystals are mounted on quartz rods and laminated with poly(methylmethacrylate) (PMMA). The experimental set-up is illustrated in Fig. S2. The number of photons absorbed by the crystals is estimated by the direct measurement of transmitted power of laser pulses through (quartz rod) – (crystal with PMMA) – (quartz rod) geometry (see Fig. S2) with Opher NOVA-display laser power meter. The quartz rod is rotated in the microwave cavity, and the changes in the effective electric field in the crystals by the rotation of the samples were calibrated based on the geometry of the crystals captured by digital CCD

camera. Because of the small size of the crystals (the maximum length of the axes was less than 1.1 mm), the calibration factors for the effective field strength were estimated less than 0.09 which is smaller than the experimental errors originated from the measurement of the number of absorbed photons (the error factor in the number was 0.2). Observed conductivity transients in the crystals are displayed in Fig. 2. The values of the conductivity in the figures are already converted into the values of  $\phi\Sigma\mu$  in equation 1 based on the number of absorbed photons estimated by the above procedure.

The values of  $\phi$  in the compounds were determined by photo-current integration with a time-of-flight measurement setup in a vacuum chamber ( $< 10^{-5}$  Pa). A planner crystal placed onto an Al electrode, and sandwiched with an ITO electrode. The surface of the crystal was illuminated by the pulses at 355 nm with the power density of  $4.4 \times 10^{16}$  photons/cm<sup>2</sup>. The inter-electrode distance was determined by an Avantes, Avaspec-2048 interferometer, determined as 24  $\mu\text{m}$ . Transient current was predominantly observed under the applied negative bias of  $0.22 - 3.3 \times 10^4$  Vcm<sup>-1</sup>, and monitored by a Tektronix TDS 3034 digitizing oscilloscope with the terminate resistance ranging from 300 – 3 k $\Omega$ . The current was also accumulated by a Keithley R6487 current integrator. The other details of the set of apparatus were described elsewhere.<sup>5</sup>

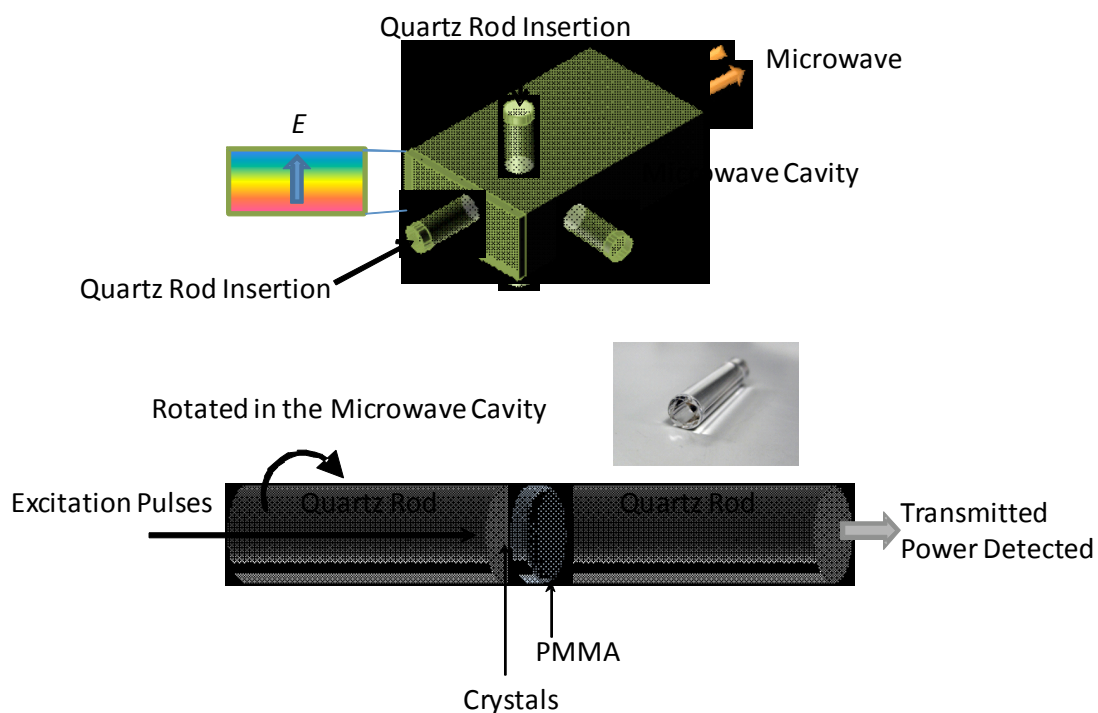


**Fig. S2** Schematic set-up of anisotropic conductivity measurements based on the time-resolved microwave conductivity (TRMC).

**Table S1.** X-ray crystallographic data for ThCBM and PCBM

|                                       | ThCBM  | PCBM   |
|---------------------------------------|--|--|
| empirical formula                     | C <sub>71.25</sub> H <sub>12</sub> O <sub>2</sub> S <sub>3.5</sub> | C <sub>146</sub> H <sub>28</sub> O <sub>3</sub> S <sub>2</sub> |
| formula weight                        | 1012.09  | 1893.80  |
| crystal system                        | triclinic  | monoclinic   |
| space group                           | <i>P</i> $\bar{1}$ (#2)  | <i>P</i> 2 <sub>1</sub> / <i>c</i> (#14)                       |
| <i>T</i> , K                          | 123  | 123  |
| <i>a</i> , Å                          | 9.9822(5)  | 10.274(2)  |
| <i>b</i> , Å                          | 16.1523(11)  | 19.101(4)  |
| <i>c</i> , Å                          | 25.744(2)  | 19.342(4)  |
| $\alpha$ , deg                        | 104.099(3)   | -  |
| $\beta$ , deg                         | 99.991(3)  | 91.6161(9)   |
| $\gamma$ , deg                        | 90.458(3)  | -  |
| <i>V</i> , Å <sup>3</sup>             | 3959.3(5)  | 3794.1(13)   |
| <i>Z</i>                              | 4  | 2  |
| no. of reflections measured           | 27288  | 29006  |
| no. of observations                   | 11236  | 8388   |
| no. of parameters refined             | 1380   | 720  |
| <i>R</i> <sub>1</sub> <sup>a</sup>    | 0.0693 ( <i>I</i> > 2σ( <i>I</i> ))                                | 0.0974 ( <i>I</i> > 2σ( <i>I</i> ))                            |
| <i>R</i> <sub>w</sub> <sup>b, c</sup> | 0.1785 (all data)  | 0.2318 (all data)  |
| GOF                                   | 1.117  | 1.098  |

<sup>a</sup>  $R_1 = \sum ||F_o| - |F_c|| / \sum |F_o|$ . <sup>b</sup>  $R_w = [\sum(\omega(F_o^2 - F_c^2)^2) / \sum\omega(F_o^2)^2]^{1/2}$ . <sup>c</sup>  $\omega = 1 / [\sigma^2(F_o^2) + (0.0500 \cdot P)^2 + 30.0000 \cdot P]$ , where  $P = (\text{Max}(F_o^2, 0) + 2F_c^2) / 3$ .

## References

- (1) *CrystalStructure* 3.8.2: Crystal Structure Analysis Package; Rigaku and Rigaku/MSO: The Woodlands, TX, 2000-2008.
- (2) M. C. Burla, R. Caliandro, M. Camalli, B. Carrozzini, G. L. Cascarano, L. de Caro, C. Giacovazzo, G. Polidori and R. Spagna, *J. Appl. Cryst.*, 2005, **38**, 381.
- (3) A. Altomare, M. C. Burla, M. Camalli, G. L. Cascarano, C. Giacovazzo, A. Guagliardi, A. G. G. Moliterni, G. Polidori and R. Spagna, *J. Appl. Cryst.*, 1999, **32**, 115.
- (4) (a) F. C. Grozema, L. D. A. Siebbeles, J. M. Warman, S. Seki, S. Tagawa and U. Scherf, *Adv. Mater.*, 2008, **14**, 228; (b) A. Acharya, S. Seki, A. Saeki, Y. Koizumi and S. Tagawa, *Chem. Phys. Lett.*, 2005, **404**, 356; (c) A. Saeki, S. Seki, T. Sunagawa, K. Ushida and S. Tagawa, *Philos. Mag.*, 2006, **86**, 1261; (d) K. Nagashima, T. Yanagida, H. Tanaka, S. Seki, A. Saeki, S. Tagawa and T. Kawai, *J. Am. Chem. Soc.*, 2008, **130**, 5378.
- (5) (a) S. Seki, Y. Yoshida, S. Tagawa, K. Asai, K. Ishigure, K. Furukawa, M. Fujiki, and N. Matsumoto, *Philos. Mag. B*, 1999, **79**, 1631; (b) H. Imahori, M. Ueda, S. Kang, H. Hayashi, S. Hayashi, H. Kaji, S. Seki, A. Saeki, S. Tagawa, T. Umeyama, Y. Matano, K. Yoshida, S. Isoda, M. Shiro, N. V. Tkachenko and H. Lemmetyinen, *Chem.–Eur. J.*, 2007, **13**, 10182; (c) I. Hisaki, Y. Sakamoto, H. Shigemitsu, N. Tohnai, M. Miyata, S. Seki, A. Saeki, and S. Tagawa, *Chem.–Eur. J.*, 2008, **14**, 4178; (d) T. Amaya, S. Seki, T. Moriuchi, K. Nakamoto, T. Nakata, H. Sakane, A. Saeki, S. Tagawa and T. Hirao, *J. Am. Chem. Soc.*, 2009, **131**, 408.